

Spinodal instabilities in nuclear matter in a stochastic relativistic mean-field approachS. Ayik,^{1,*} O. Yilmaz,² N. Er,² A. Gokalp,² and P. Ring³¹*Physics Department, Tennessee Technological University, Cookeville, Tennessee 38505, USA*²*Physics Department, Middle East Technical University, 06531 Ankara, Turkey*³*Physics Department, TU Munich, D-85748 Garching, Germany*

(Received 8 July 2009; published 21 September 2009)

Spinodal instabilities and early growth of baryon density fluctuations in symmetric nuclear matter are investigated in the basis of the stochastic extension of the relativistic mean-field approach in the semiclassical approximation. Calculations are compared with the results of nonrelativistic calculations based on Skyrme-type effective interactions under similar conditions. A qualitative difference appears in the unstable response of the system: the system exhibits most unstable behavior at higher baryon densities around $\rho_b = 0.4\rho_0$ in the relativistic approach while most unstable behavior occurs at lower baryon densities around $\rho_b = 0.2\rho_0$ in the nonrelativistic calculations

DOI: [10.1103/PhysRevC.80.034613](https://doi.org/10.1103/PhysRevC.80.034613)

PACS number(s): 24.10.Jv, 21.30.Fe, 21.65.-f, 26.60.-c

I. INTRODUCTION

Spinodal instability provides a possible dynamical mechanism for fragmentation of a hot piece of nuclear matter produced in heavy-ion collisions. Small amplitude density fluctuations grow rapidly and lead to the breakup of the system into an ensemble of clusters [1]. In the coming years, experimental investigations of multifragmentation reactions in a neutron rich nuclear system will provide a further understanding of the isospin dependence of a nuclear matter equation of state at low densities. On the theoretical side, extensive investigations of spinodal instabilities have been carried out in the basis of stochastic transport models [2–6]. In particular, the recently proposed stochastic mean-field approach provides us with a useful tool for a description of dynamics of density fluctuations in the spinodal region [7]. It has been demonstrated that the stochastic mean-field approach incorporates the one-body dissipation and the associated fluctuation mechanism in accordance with the quantal-dissipation fluctuation relation. The approach gives rise to the same result for the dispersion of one-body observables that was obtained in a variational approach in a previous work [8]. Furthermore, in recent studies [9,10] by projecting onto macroscopic variables, we deduce transport coefficients for energy dissipation and nucleon exchange in low-energy heavy-ion collisions, which have a similar form to those familiar with the phenomenological nucleon exchange model [11]. These investigations provide a strong support for the fact that the stochastic mean-field approach is a powerful tool for describing low-energy nuclear collisions and spinodal dynamics.

In a recent work, we studied the early development of spinodal dynamics of nuclear matter in the basis of the stochastic mean-field approach by employing density-dependent Skyrme-type effective interactions [12]. In the present work, we carry out a similar investigation of early development of density fluctuations in the spinodal region of nuclear matter by employing the stochastic extension of the

relativistic mean-field theory [13,14]. It has been shown in recent years that the nuclear many-body system is in principal a relativistic system driven by dynamics of large relativistic attractive scalar and repulsive vector fields. Both fields are not much smaller than the nucleon mass and therefore the average nuclear field should be described by the Dirac equation. For large components of Dirac spinors, two fields nearly cancel each other leading to a relatively small attractive mean field. The small components add up leading to a very large spin orbit term, which was known since the early days of nuclear physics. Relativistic models have been used with great success to describe nuclear structure. In recent years, the approach was also applied for the description of nuclear dynamics extended in the framework of time-dependent covariant density functional theory [15,16]. A number of investigations have been carried out on spinodal instabilities in nuclear matter employing relativistic mean-field approaches [17–19]. In this work, we consider the stochastic extension of the relativistic mean-field theory in the semiclassical approximation. As illustrated in the nonrelativistic limit, stochastic extension of the mean-field theory provides a powerful approach for investigating dynamics of density fluctuations. Employing the stochastic extension of the relativistic mean-field approach, we investigate not only spinodal instabilities but also the early development of density fluctuations in symmetric nuclear matter.

In Sec. II, we briefly describe the stochastic extension of the relativistic mean-field theory in the semiclassical approximation. In Sec. III, we calculate the early growth of baryon density fluctuations, growth rates, and the phase diagram of dominant modes in symmetric nuclear matter. Conclusions are given in Sec. IV.

II. STOCHASTIC RELATIVISTIC MEAN-FIELD THEORY

The stochastic mean-field approach is based on a very appealing stochastic model proposed for describing deep-inelastic heavy-ion collisions and sub-barrier fusion [20–22]. In that model, dynamics of relative motion is coupled to

* ayik@tntech.edu

collective surface modes of colliding ions and treated in a classical framework. The initial quantum zero point and thermal fluctuations are incorporated into the calculations in a stochastic manner by generating an ensemble of events according to the initial distribution of collective modes. In the mean-field evolution, couplings of relative motion with all other collective and noncollective modes are automatically taken into account. In the stochastic extension of the mean-field approach, the zero point and thermal fluctuations of the initial state are taken into account in a stochastic manner, in a similar manner as presented in Refs. [20–22]. The initial fluctuations, which are specified by a specific Gaussian random ensemble, are simulated by considering the evolution of an ensemble of single-particle density matrices. It is possible to incorporate quantal and thermal fluctuations of the initial state into the relativistic mean-field description in a similar manner.

In Refs. [23,24], the authors derived a relativistic Vlasov equation from the Walecka model in the local density and the semiclassical approximation. In the Walecka model, the interaction between nucleons is mediated by a scalar meson with mass m_s , and a vector meson with mass m_v , with respective fields denoted as ϕ and V_μ . Introducing the phase space distribution function $f(\vec{r}, \vec{p}, t)$ for the nucleons, the following relativistic Vlasov equation has been obtained:

$$\frac{\partial}{\partial t} f(\vec{r}, \vec{p}, t) + \vec{v} \cdot \vec{\nabla}_r f(\vec{r}, \vec{p}, t) - \vec{\nabla}_r h(\vec{r}, \vec{p}) \cdot \vec{\nabla}_p f(\vec{r}, \vec{p}, t) = 0, \quad (1)$$

where $\vec{v} = \vec{p}^*/e^*$ and $h = e^* + g_v V_0$. The coupling constants of the mesons and the nucleon are denoted by g_s and g_v for the scalar and the vector mesons, respectively. In these expressions, $\vec{p}^* = \vec{p} - g_v \vec{V}$ and $e^* = (\vec{p}^{*2} + M^{*2})^{1/2}$ with $M^* = M - g_s \phi$. The nucleon mass is denoted by M . In the mean-field approximation, the meson fields are treated as classical fields and their evolutions are determined by the field equations

$$\left[\frac{\partial^2}{\partial t^2} - \nabla^2 + m_s^2 \right] \phi(\vec{r}, t) = g_s \rho_s(\vec{r}, t) \quad (2)$$

and

$$\left[\frac{\partial^2}{\partial t^2} - \nabla^2 + m_v^2 \right] V_\nu(\vec{r}, t) = g_v \rho_\nu(\vec{r}, t). \quad (3)$$

In these expressions, the baryon density $\rho_0(\vec{r}, t) = \rho_b(\vec{r}, t)$, the scalar density $\rho_s(\vec{r}, t)$, and the current density $\vec{\rho}_v(\vec{r}, t)$ can be expressed in terms of phase-space distribution function as follows:

$$\rho_b(\vec{r}, t) = \gamma \int \frac{d^3 p}{(2\pi)^3} f(\vec{r}, \vec{p}, t), \quad (4)$$

$$\rho_s(\vec{r}, t) = \gamma \int \frac{d^3 p}{(2\pi)^3} \frac{M^*}{e^*} f(\vec{r}, \vec{p}, t), \quad (5)$$

and

$$\vec{\rho}_v(\vec{r}, t) = \gamma \int \frac{d^3 p}{(2\pi)^3} \frac{\vec{p}^*}{e^*} f(\vec{r}, \vec{p}, t), \quad (6)$$

where $\gamma = 4$ is the spin-isospin degeneracy factor. The original Walecka model gives a nuclear compressibility that is

much larger than the one extracted from the giant monopole resonances in nuclei. It also leads to an effective nucleon mass which is smaller than the value determined from the analysis of nucleon-nucleus scattering. In order to have a model which allows different values of nuclear compressibility and the nucleon effective mass, it is possible to improve the Walecka model by including the self-interaction of the scalar mesons or by considering density dependent coupling constants. However, in the present exploratory work, we employ the original Walecka model without including the self-interaction of the scalar meson.

In the stochastic mean-field approach an ensemble $\{f^\lambda(\vec{r}, \vec{p}, t)\}$ of the phase-space distributions is generated in accordance with the initial fluctuations, where λ indicates the event label. In the following, for simplicity of notation, since equations of motion do not change in the stochastic evolution, we do not use the event label λ for the phase-space distributions and also for the other quantities. However it is understood that the phase-space distribution, scalar meson, and vector meson fields are fluctuating quantities. Each member of the ensemble of phase-space distributions evolves by the same Vlasov [1] equation according to its own self-consistent mean field, but with different initial conditions. The main assumption of the approach in the semiclassical representation is the following: In each phase-space cell, the initial phase-space distribution $f(\vec{r}, \vec{p}, 0)$ is a Gaussian random number with its mean value determined by $\overline{f(\vec{r}, \vec{p}, 0)} = f_0(\vec{r}, \vec{p})$, and its second moment is determined by [7,12]

$$\overline{f(\vec{r}, \vec{p}, 0) f(\vec{r}', \vec{p}', 0)} = (2\pi)^3 \delta(\vec{r} - \vec{r}') \delta(\vec{p} - \vec{p}') f_0(\vec{r}, \vec{p}) [1 - f_0(\vec{r}, \vec{p})], \quad (7)$$

where the overline represents the ensemble averaging and $f_0(\vec{r}, \vec{p})$ denotes the average phase-space distribution describing the initial state. In the special case of a homogenous initial state, it is given by the Fermi-Dirac distribution $f_0(p) = 1/[\exp(e_0^* - \mu_0^*)/T + 1]$. In this expression $\mu_0^* = \mu_0 - (g_v/m_v)^2 \rho_b^0$, where μ_0 is the chemical potential and ρ_b^0 is the baryon density in the homogenous initial state.

In this work, we investigate the early growth of density fluctuations in the spinodal region in symmetric nuclear matter. For this purpose, it is sufficient to consider the linear response treatment of dynamical evolution. The small amplitude fluctuations of the phase-space distribution $\delta f(\vec{r}, \vec{p}, t) = f(\vec{r}, \vec{p}, t) - f_0(\vec{p})$ around an equilibrium state $f_0(\vec{p})$ are determined by the linearized Vlasov equation,

$$\frac{\partial}{\partial t} \delta f(\vec{r}, \vec{p}, t) + \vec{v}_0 \cdot \vec{\nabla}_r \delta f(\vec{r}, \vec{p}, t) - \vec{\nabla}_r \delta h(\vec{r}, \vec{p}, t) \cdot \vec{\nabla}_p f_0(p) = 0. \quad (8)$$

In this expression the local velocity is $\vec{v}_0 = \vec{p}/e_0^*$ with $e_0^* = \sqrt{\vec{p}^2 + M_0^{*2}}$, $M_0^* = M - g_s \phi_0$, and small fluctuations of the mean-field Hamiltonian is given by

$$\delta h(\vec{r}, \vec{p}, t) = -\frac{M_0^*}{e_0^*} g_s \delta \phi(\vec{r}, t) + g_v \delta V_0(\vec{r}, t) - \frac{g_v}{e_0^*} \vec{p} \cdot \delta \vec{V}(\vec{r}, t). \quad (9)$$

The small fluctuations of the scalar and vector mesons are determined by the linearized field equations,

$$\left[\frac{\partial^2}{\partial t^2} - \nabla^2 + m_s^2 \right] \delta\phi(\vec{r}, t) = g_s \delta\rho_s(\vec{r}, t) \quad (10)$$

and

$$\left[\frac{\partial^2}{\partial t^2} - \nabla^2 + m_v^2 \right] \delta V_v(\vec{r}, t) = g_v \delta\rho_v(\vec{r}, t). \quad (11)$$

III. EARLY GROWTH OF DENSITY FLUCTUATIONS

A. Spinodal instabilities

In this section, we employ the stochastic relativistic mean-field approach in the small amplitude limit to investigate spinodal instabilities in symmetric nuclear matter. We can obtain the solution of linear response Eqs. (7)–(11) by employing the standard method of the one-sided Fourier transform in time [25]. It is also convenient to introduce the Fourier transform of the phase-space distribution in space,

$$\delta\tilde{f}(\vec{k}, \vec{p}, \omega) = \int_0^\infty dt e^{i\omega t} \int_{-\infty}^\infty d^3r e^{-i\vec{k}\cdot\vec{r}} f(\vec{r}, \vec{p}, t). \quad (12)$$

This leads to

$$\begin{aligned} \delta\tilde{f}(\vec{k}, \vec{p}, \omega) = & \left(\frac{M_0^*}{e_0^*} \tilde{g}_s^2 \delta\tilde{\rho}_s(\vec{k}, \omega) - \tilde{g}_v^2 \delta\tilde{\rho}_b(\vec{k}, \omega) \right. \\ & + \tilde{g}_v^2 \frac{\vec{p}}{e_0^*} \cdot \delta\tilde{\rho}_v(\vec{k}, \omega) \left. \right) \frac{\vec{k} \cdot \vec{\nabla}_p f_0(p)}{\omega - \vec{v}_0 \cdot \vec{k}} \\ & + i \frac{\delta\tilde{f}(\vec{k}, \vec{p}, 0)}{\omega - \vec{v}_0 \cdot \vec{k}}, \end{aligned} \quad (13)$$

where $\delta\tilde{f}(\vec{k}, \vec{p}, 0)$ denotes the Fourier transform of the initial fluctuations, and we use the short-hand notation, $\tilde{g}_s^2 = g_s^2/(k^2 + m_s^2)$, $\tilde{g}_v^2 = g_v^2/(k^2 + m_v^2)$. In this expression, the fluctuations of the meson fields are expressed in terms of Fourier transforms of the scalar density $\delta\rho_s(\vec{r}, t)$, the baryon density $\delta\rho_b(\vec{r}, t)$, and the current density $\delta\rho_v(\vec{r}, t)$ fluctuations by employing the field Eqs. (10) and (11). In Eq. (13) only the initial fluctuations of the phase-space distribution $\delta\tilde{f}(\vec{k}, \vec{p}, 0)$ are kept, but the initial fluctuations associated with the scalar and the vector fields are neglected. In the spinodal region since it is expected to have a small contribution, we neglect the frequency terms in the propagators, i.e., $-\omega^2 + k^2 + m_s^2 \approx k^2 + m_s^2$ and $-\omega^2 + k^2 + m_v^2 \approx k^2 + m_v^2$. Small fluctuations of the baryon density, the scalar density, and the current density are related to the fluctuation of the phase-space distribution function $\delta\tilde{f}(\vec{k}, \vec{p}, \omega)$ according to

$$\begin{aligned} \delta\tilde{\rho}_b(\vec{k}, \omega) &= \gamma \int \frac{d^3p}{(2\pi)^3} \delta\tilde{f}(\vec{k}, \vec{p}, \omega), \quad (14) \\ \delta\tilde{\rho}_s(\vec{k}, \omega) &= \gamma \int \frac{d^3p}{(2\pi)^3} \left[\delta \left(\frac{M^*}{e^*} \right) f_0(p) + \frac{M_0^*}{e_0^*} \delta\tilde{f}(\vec{k}, \vec{p}, \omega) \right] \end{aligned}$$

$$\begin{aligned} &= \gamma \int \frac{d^3p}{(2\pi)^3} \left[\left(\tilde{g}_v^2 \frac{M_0^*}{e_0^{*3}} \vec{p} \cdot \delta\tilde{\rho}_v(\vec{k}, \omega) \right. \right. \\ &\quad \left. \left. - \tilde{g}_s^2 \frac{p^2}{e_0^{*3}} \delta\tilde{\rho}_s(\vec{k}, \omega) \right) f_0(p) + \frac{M_0^*}{e_0^*} \delta\tilde{f}(\vec{k}, \vec{p}, \omega) \right], \end{aligned} \quad (15)$$

and

$$\begin{aligned} \delta\tilde{\rho}_v(\vec{k}, \omega) &= \gamma \int \frac{d^3p}{(2\pi)^3} \left[\delta \left(\frac{\vec{p}^*}{e^*} \right) f_0(p) + \frac{\vec{p}}{e_0^*} \delta\tilde{f}(\vec{k}, \vec{p}, \omega) \right] \\ &= \gamma \int \frac{d^3p}{(2\pi)^3} \left[\left(\tilde{g}_v^2 \frac{\vec{p}}{e_0^{*3}} \vec{p} \cdot \delta\tilde{\rho}_v(\vec{k}, \omega) \right. \right. \\ &\quad \left. \left. - \tilde{g}_v^2 \frac{\delta\tilde{\rho}_v(\vec{k}, \omega)}{\epsilon_0^*} + \tilde{g}_s^2 \frac{M_0^*}{e_0^{*3}} \vec{p} \delta\tilde{\rho}_s(\vec{k}, \omega) \right) \right. \\ &\quad \left. \times f_0(p) + \frac{\vec{p}}{\epsilon_0^*} \delta\tilde{f}(\vec{k}, \vec{p}, \omega) \right]. \end{aligned} \quad (16)$$

Multiplying both sides of Eq. (13) by M_0^*/e_0^* , 1 , \vec{p}/e_0^* and integrating over the momentum, we deduce a set of coupled algebraic equations for the small fluctuations of the scalar density, the baryon density, and the current density, which can be put in to a matrix form. Here we investigate spinodal dynamics of the longitudinal unstable modes. For longitudinal modes the current density oscillates along the direction of propagation, $\delta\tilde{\rho}_v(\vec{k}, \omega) = \delta\tilde{\rho}_v(\vec{k}, \omega)\hat{k}$. Then, for the longitudinal modes, the set of equations becomes

$$\begin{pmatrix} A_1 & A_2 & A_3 \\ B_1 & B_2 & B_3 \\ C_1 & C_2 & C_3 \end{pmatrix} \begin{pmatrix} \delta\tilde{\rho}_v(\vec{k}, \omega) \\ \delta\tilde{\rho}_s(\vec{k}, \omega) \\ \delta\tilde{\rho}_b(\vec{k}, \omega) \end{pmatrix} = i \begin{pmatrix} \tilde{S}_b(\vec{k}, \omega) \\ \tilde{S}_s(\vec{k}, \omega) \\ \tilde{S}_v(\vec{k}, \omega) \end{pmatrix}, \quad (17)$$

where the element of the coefficient matrix are defined according to

$$\begin{pmatrix} A_1 & A_2 & A_3 \\ B_1 & B_2 & B_3 \\ C_1 & C_2 & C_3 \end{pmatrix} = \begin{pmatrix} -\tilde{g}_v^2 \chi_v(\vec{k}, \omega) & -\tilde{g}_s^2 \chi_s(\vec{k}, \omega) & 1 + \tilde{g}_v^2 \chi_b(\vec{k}, \omega) \\ -\tilde{g}_v^2 \tilde{\chi}_v(\vec{k}, \omega) & 1 + \tilde{g}_s^2 \tilde{\chi}_s(\vec{k}, \omega) & \tilde{g}_v^2 \chi_s(\vec{k}, \omega) \\ 1 + \tilde{g}_v^2 \tilde{\chi}_b(\vec{k}, \omega) & -\tilde{g}_s^2 \chi_v(\vec{k}, \omega) & \tilde{g}_v^2 \chi_v(\vec{k}, \omega) \end{pmatrix}. \quad (18)$$

In this expression, $\chi_b(\vec{k}, \omega)$, $\chi_s(\vec{k}, \omega)$, and $\chi_v(\vec{k}, \omega)$ denote the long wavelength limit of relativistic Lindhard functions associated with baryon, scalar, and current density distribution functions,

$$\begin{pmatrix} \chi_v(\vec{k}, \omega) \\ \chi_s(\vec{k}, \omega) \\ \chi_b(\vec{k}, \omega) \end{pmatrix} = \gamma \int \frac{d^3p}{(2\pi\hbar)^3} \begin{pmatrix} \vec{p} \cdot \hat{k}/e_0^* \\ M_0^*/e_0^* \\ 1 \end{pmatrix} \frac{\vec{k} \cdot \vec{\nabla}_p f_0(p)}{\omega - \vec{v}_0 \cdot \vec{k}}, \quad (19)$$

and the stochastic source terms are determined by

$$\begin{pmatrix} \tilde{S}_b(\vec{k}, \omega) \\ \tilde{S}_s(\vec{k}, \omega) \\ \tilde{S}_v(\vec{k}, \omega) \end{pmatrix} = \gamma \int \frac{d^3 p}{(2\pi)^3} \begin{pmatrix} 1 \\ M_0^*/e_0^* \\ \vec{p} \cdot \hat{k}/e_0^* \end{pmatrix} \frac{\delta \tilde{f}(\vec{k}, \vec{p}, 0)}{\omega - \vec{v}_0 \cdot \vec{k}}. \quad (20)$$

The other three elements of the coefficient matrix in Eq. (18) are given by

$$\tilde{\chi}_s(\vec{k}, \omega) = \gamma \int \frac{d^3 p}{(2\pi)^3} \left[\frac{p^2}{e_0^{*3}} f_0(p) - \frac{M_0^{*2}}{e_0^{*2}} \frac{\vec{k} \cdot \vec{\nabla}_p f_0(p)}{\omega - \vec{v}_0 \cdot \vec{k}} \right], \quad (21)$$

$$\tilde{\chi}_v(\vec{k}, \omega) = \gamma \int \frac{d^3 p}{(2\pi)^3} \vec{p} \cdot \hat{k} \left[\frac{M_0^*}{e_0^{*2}} \frac{\vec{k} \cdot \vec{\nabla}_p f_0(p)}{\omega - \vec{v}_0 \cdot \vec{k}} \right], \quad (22)$$

and

$$\begin{aligned} \tilde{\chi}_b(\vec{k}, \omega) = \gamma \int \frac{d^3 p}{(2\pi)^3} & \left[\frac{e_0^{*2} - (\vec{p} \cdot \hat{k})^2}{e_0^{*3}} f_0(p) \right. \\ & \left. - \frac{(\vec{p} \cdot \hat{k})^2}{e_0^{*2}} \frac{\vec{k} \cdot \vec{\nabla}_p f_0(p)}{\omega - \vec{v}_0 \cdot \vec{k}} \right]. \end{aligned} \quad (23)$$

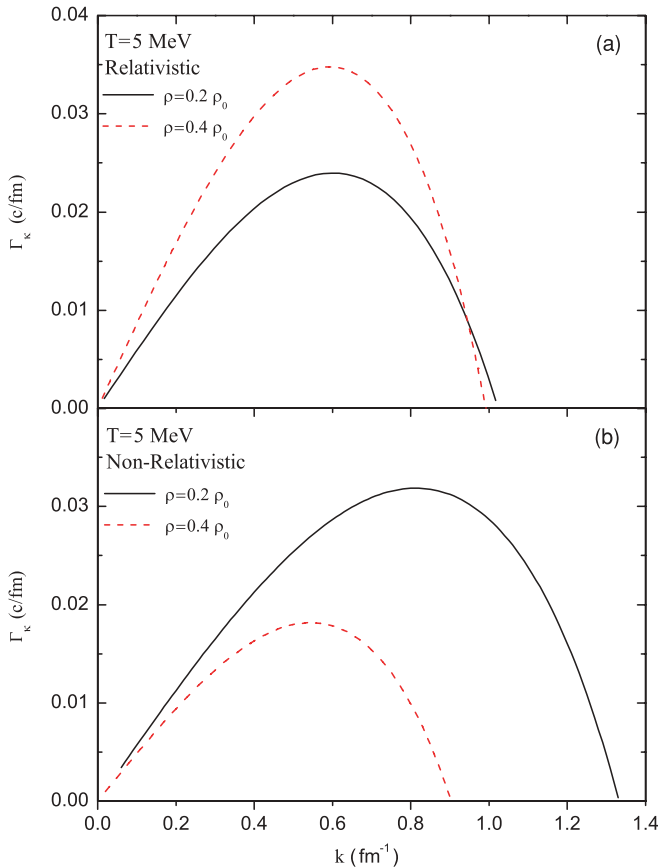


FIG. 1. (Color online) Growth rates of unstable modes as a function of wave numbers in the spinodal region at baryon densities $\rho_b = 0.2\rho_0$ and $\rho_b = 0.4\rho_0$ at temperature $T = 5$ MeV: (a) relativistic calculations, and (b) nonrelativistic calculations.

We obtain the solutions by inverting the algebraic matrix equation, which gives, for the baryon density fluctuations,

$$\delta \tilde{\rho}_B(\vec{k}, \omega) = i \frac{D_1 \tilde{S}_b(\vec{k}, \omega) + D_2 \tilde{S}_s(\vec{k}, \omega) + D_3 \tilde{S}_v(\vec{k}, \omega)}{\varepsilon(\vec{k}, \omega)}, \quad (24)$$

where $D_1 = B_1 C_2 - B_2 C_1$, $D_2 = C_1 A_2 - C_2 A_1$, and $D_3 = A_1 B_2 - A_2 B_1$ and the quantity $\varepsilon(k, \omega) = A_3 D_1 + B_3 D_2 + C_3 D_3$ denotes the susceptibility.

The evolution in time is determined by taking the inverse Fourier transformation in time, which can be calculated with the help of the residue theorem [24]. Keeping only the growing and decaying collective poles, we find

$$\delta \tilde{\rho}_b(\vec{k}, t) = \delta \rho_b^+(\vec{k}) e^{+\Gamma_k t} + \delta \rho_b^-(\vec{k}) e^{-\Gamma_k t}. \quad (25)$$

Here, the amplitudes of baryon density fluctuations associated with the growing and decaying modes at the initial instant are given by

$$\begin{aligned} \delta \rho_b^\mp(\vec{k}) &= - \left\{ \frac{D_1 \tilde{S}_b(\vec{k}, \omega) + D_2 \tilde{S}_s(\vec{k}, \omega) + D_3 \tilde{S}_v(\vec{k}, \omega)}{\partial \varepsilon(\vec{k}, \omega) / \partial \omega} \right\}_{\omega = \mp i \Gamma_k} \end{aligned} \quad (26)$$

The growth and decay rates of the modes are obtained from the dispersion relations, $\varepsilon(\vec{k}, \omega) = 0$, i.e., from the roots of susceptibility. Solutions for the scalar density fluctuations $\delta \tilde{\rho}_s(\vec{k}, \omega)$ and the current density $\delta \tilde{\rho}_v(\vec{k}, \omega)$ fluctuations can be expressed in a similar manner. In the original Walecka model, there are four free parameters, coupling constants, and meson masses. The binding energy per nucleon at saturation density determines the ratios of coupling constants to masses. The standard values of the ratios $g_v^2(M/m_v)^2 = 273.8$ and

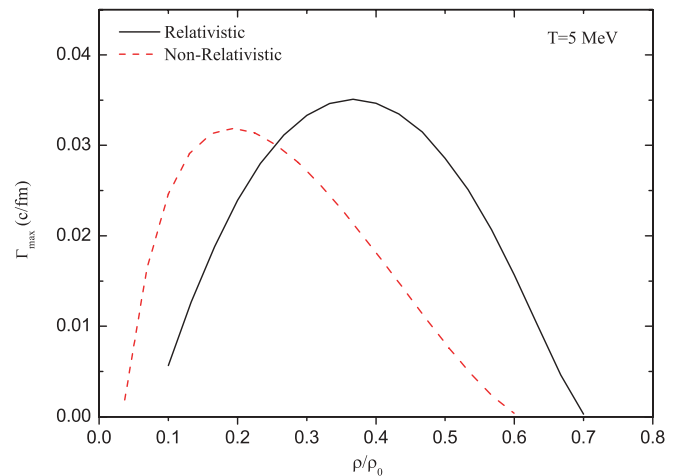


FIG. 2. (Color online) Growth rates of the most unstable modes as function of baryon density in the spinodal region at temperature $T = 5$ MeV in relativistic calculations (solid line) and in nonrelativistic calculations (dashed line).

$g_s^2(M/m_s)^2 = 357.4$ give the binding energy per nucleon as 15.75 MeV at saturation density [13,14]. These ratios lead to an effective nucleon mass $M_0^* = 0.541 M$ and a compressibility of 540 MeV at the saturation density. In numerical calculations, we take the vector meson mass $m_v = 783$ MeV, and the scalar meson mass $m_s = 500$ MeV. As an example, the upper panel in Fig. 1 shows the growth rates of unstable modes as a function of wave number in the spinodal region corresponding to the initial baryon density $\rho_b = 0.2\rho_0$ and $\rho_b = 0.4\rho_0$ at a temperature $T = 5$ MeV. The lower panel of Fig. 1 illustrates the dispersion relations obtained in the nonrelativistic approach with an effective Skyrme force [12]. Although a direct comparison of these calculations is rather difficult, we observe that there are qualitative differences in both calculations. The range of most unstable modes in relativistic calculations is concentrated around $k = 0.6 \text{ fm}^{-1}$ in both densities, while most unstable modes shift toward larger wave numbers around $k = 0.8 \text{ fm}^{-1}$ at density $\rho_b = 0.2\rho_0$ and toward smaller wave numbers around $k = 0.5 \text{ fm}^{-1}$ at density $\rho_b = 0.4\rho_0$. Growth rates of most unstable modes at density $\rho_b = 0.4\rho_0$ in relativistic calculations are nearly a factor of two larger than those results obtained in the nonrelativistic calculations, while at low density $\rho_b = 0.2\rho_0$ the growth rates are smaller in relativistic calculations. Figure 2 illustrates growth rates of the most unstable modes as a function of density in both relativistic and nonrelativistic approaches. We observe the qualitative difference in the unstable response of the system: the system exhibits most unstable behavior at higher densities around $\rho_b = 0.4\rho_0$ in the relativistic approach while most unstable behavior occurs in the nonrelativistic calculations at lower densities around $\rho_b = 0.2\rho_0$. As an example of phase diagrams, Fig. 3 shows the boundary of the spinodal region for the unstable mode of the wavelength $\lambda = 9.0$ fm. Again, we observe that the unstable behavior shifts toward higher densities in relativistic calculations.

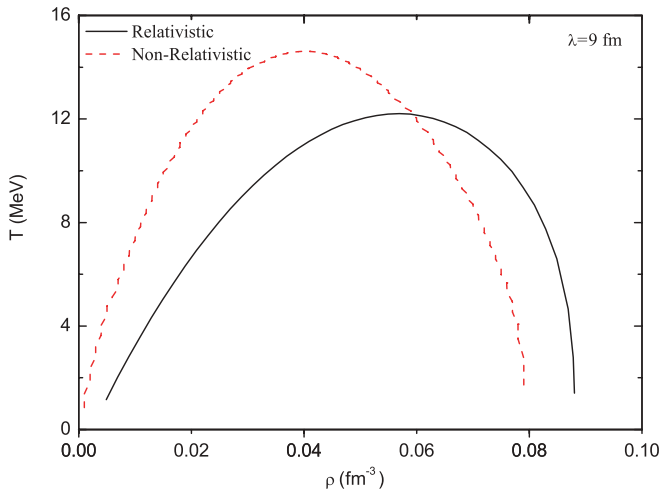


FIG. 3. (Color online) Boundary of the spinodal region in the baryon density-temperature plane for the unstable mode with wavelengths $\lambda = 9$ fm in relativistic calculations (solid line) and in nonrelativistic calculations (dashed line).

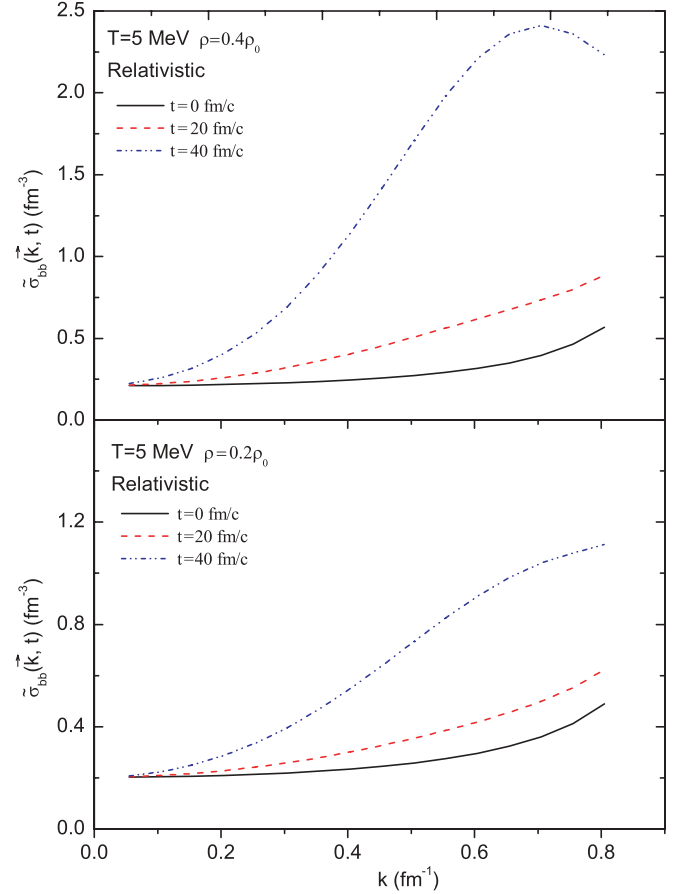


FIG. 4. (Color online) Spectral intensity $\tilde{\sigma}_b(\vec{k}, t)$ of the baryon density correlation function as a function of wave number at times $t = 0, t = 20 \text{ fm/c}$ and $t = 40 \text{ fm/c}$ at temperature $T = 5$ MeV in relativistic calculations at densities (a) $\rho_b = 0.2\rho_0$ and (b) $\rho_b = 0.4\rho_0$.

B. Growth of density fluctuations

In this section, we calculate the early growth of baryon density fluctuations in nuclear matter. The spectral intensity of the density correlation function $\tilde{\sigma}_{bb}(\vec{k}, t)$ is related to the variance of the Fourier transform of baryon density fluctuation according to

$$\tilde{\sigma}_{bb}(\vec{k}, t)(2\pi)^3 \delta(\vec{k} - \vec{k}') = \overline{\delta\tilde{\rho}_b(\vec{k}, t)\delta\tilde{\rho}_b^*(\vec{k}', t)}. \quad (27)$$

We calculate the spectral function using the solution (25) and the expression (7) for the initial fluctuations to give

$$\tilde{\sigma}_{bb}(\vec{k}, t) = \frac{E_b^+(\vec{k})}{|[\partial\epsilon(\vec{k}, \omega)/\partial\omega]_{\omega=i\Gamma_k}|^2} (e^{2\Gamma_k t} + e^{-2\Gamma_k t}) + \frac{2E_b^-(\vec{k})}{|[\partial\epsilon(\vec{k}, \omega)/\partial\omega]_{\omega=i\Gamma_k}|^2}, \quad (28)$$

where

$$E_b^\mp(\vec{k}) = |D_1|^2 K_{11}^\mp + |D_2|^2 K_{22}^\mp \mp |D_3|^2 K_{33}^\mp + 2D_1 D_2 K_{12}^\mp \quad (29)$$

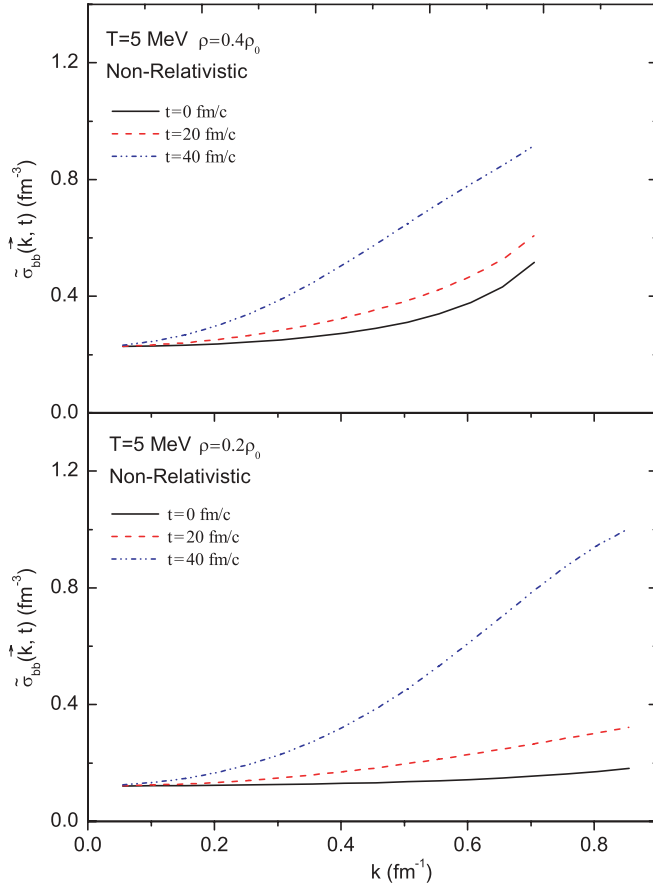


FIG. 5. (Color online) Same as Fig. 4 in nonrelativistic calculations.

with

$$K_{11}^{\mp} = \gamma^2 \int \frac{d^3 p}{(2\pi)^3} \frac{\Gamma_k^2 \mp (\vec{v}_0 \cdot \vec{k})^2}{[\Gamma_k^2 + (\vec{v}_0 \cdot \vec{k})^2]^2} f_0(p)[1 - f_0(p)], \quad (30)$$

$$K_{22}^{\mp} = \gamma^2 \int \frac{d^3 p}{(2\pi)^3} \left(\frac{M_0^*}{e_0^*} \right)^2 \frac{\Gamma_k^2 \mp (\vec{v}_0 \cdot \vec{k})^2}{[\Gamma_k^2 + (\vec{v}_0 \cdot \vec{k})^2]^2} \times f_0(p)[1 - f_0(p)], \quad (31)$$

$$K_{33}^{\mp} = \gamma^2 \int \frac{d^3 p}{(2\pi)^3} \left(\frac{\vec{p} \cdot \vec{k}}{e_0^*} \right)^2 \frac{\Gamma_k^2 \mp (\vec{v}_0 \cdot \vec{k})^2}{[\Gamma_k^2 + (\vec{v}_0 \cdot \vec{k})^2]^2} \times f_0(p)[1 - f_0(p)], \quad (32)$$

and

$$K_{12}^{\mp} = \gamma^2 \int \frac{d^3 p}{(2\pi)^3} \frac{M_0^*}{e_0^*} \frac{\Gamma_k^2 \mp (\vec{v}_0 \cdot \vec{k})^2}{[\Gamma_k^2 + (\vec{v}_0 \cdot \vec{k})^2]^2} \times f_0(p)[1 - f_0(p)]. \quad (33)$$

The upper and lower panels of Fig. 4 show the spectral intensity of the baryon density correlation function as a function of wave number at times $t = 0$, $t = 20$ fm/c, and $t = 40$ fm/c at temperature $T = 5$ MeV in relativistic calculations at densities $\rho_b = 0.2\rho_0$ and $\rho_b = 0.4\rho_0$, respectively. We observe that the largest growth occurs over the range of wave numbers corresponding to the range of dominant

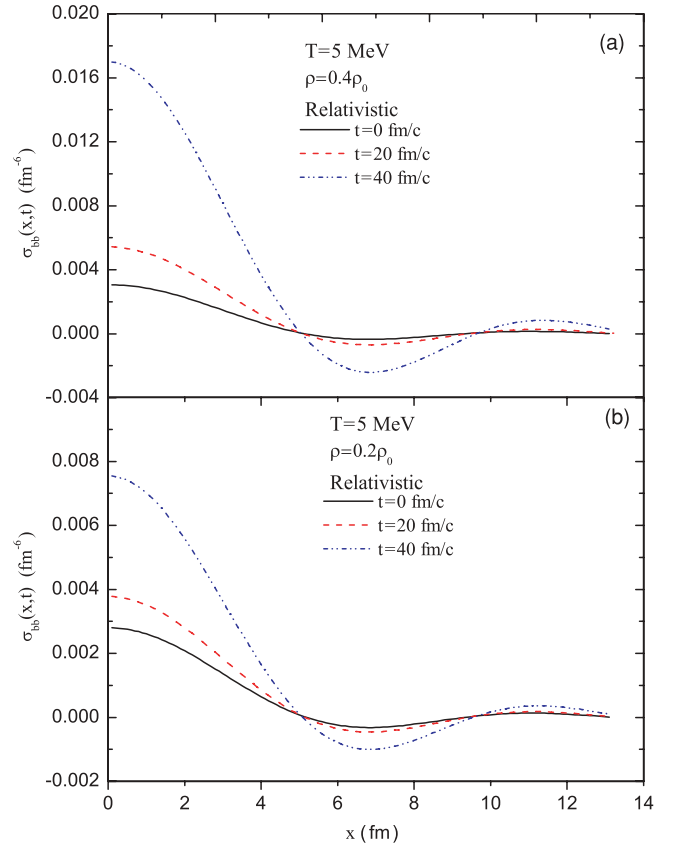


FIG. 6. (Color online) Baryon density correlation function $\sigma_b(x, t)$ as a function of distance $x = |\vec{r} - \vec{r}'|$ between two space points at times $t = 0$, $t = 20$ fm/c and $t = 40$ fm/c at temperature $T = 5$ MeV in relativistic calculations at densities (a) $\rho_b = 0.2\rho_0$ and (b) $\rho_b = 0.4\rho_0$.

unstable modes. Spectral intensity in the vicinity of most unstable modes of $k = 0.6$ fm $^{-1}$ grows about a factor of ten at density $\rho_b = 0.2\rho_0$ and about a factor of six at density $\rho_b = 0.4\rho_0$ during the time interval of $t = 40$ fm/c. Figure 5 shows similar information calculated in the nonrelativistic approaches. We notice that at density $\rho_b = 0.2\rho_0$ the behavior of the spectral intensity is rather similar in relativistic and nonrelativistic approaches. However, at higher density $\rho_b = 0.4\rho_0$, the spectral intensity grows slower in the nonrelativistic calculations than those obtained in the relativistic approach. We note that in determining time evolution $\delta\rho_b(\vec{k}, t)$ with the help of the residue theorem, there are other contributions arising from the noncollective pole of the susceptibility $\varepsilon(\vec{k}, \omega)$ and from the poles of source terms $\tilde{S}_v(\vec{k}, \omega)$, $\tilde{S}_s(\vec{k}, \omega)$, and $\tilde{S}_b(\vec{k}, \omega)$. These contributions, in particular toward the short wavelengths, i.e., toward higher wave numbers, are important at the initial stage, however they dampen out in a short time interval [25]. Since, we do not include effects from noncollective poles, we terminate the spectral in Fig. 5 at a cut-off wave number $k_c \approx 0.7$ fm $^{-1}$ – 0.8 fm $^{-1}$. Consequently, the expression (28) provides a good approximation for $\tilde{\sigma}_{bb}(\vec{k}, t)$ in the long wavelength regime below k_c .

Local baryon density fluctuations $\delta\rho_b(\vec{r}, t)$ are determined by the Fourier transform of $\delta\rho_b(\vec{k}, t)$. An equal time correlation

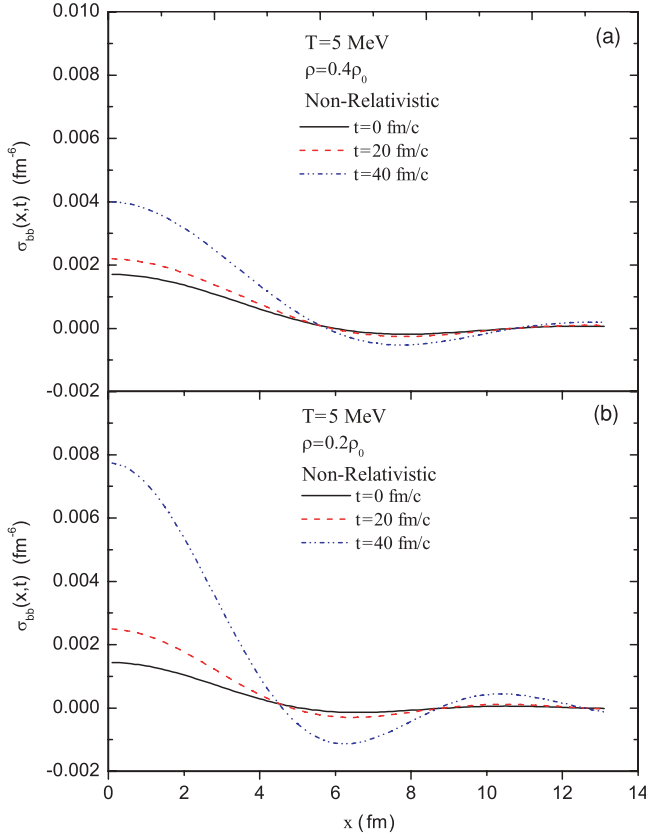


FIG. 7. (Color online) Same as Fig. 6 in nonrelativistic calculations.

function of baryon density fluctuations as a function of distance between two space locations can be expressed in terms of the spectral intensity as

$$\sigma_{bb}(|\vec{r} - \vec{r}'|, t) = \overline{\delta\rho_b(\vec{r}, t)\delta\rho_b(\vec{r}', t)} = \int \frac{d^3k}{(2\pi)^3} e^{i\vec{k}\cdot\vec{r}} \tilde{\sigma}_{bb}(\vec{k}, t). \quad (34)$$

The baryon density correlation function carries useful information about the unstable dynamics of the matter in the spinodal region. As an example, the upper and lower panels of Fig. 6 illustrates the baryon density correlation function as a function distance between two space points at times $t = 0$, $t = 20$ fm/c, and $t = 40$ fm/c at temperature $T = 5$ MeV in relativistic calculations at densities $\rho_b = 0.4\rho_0$ and $\rho_b = 0.2\rho_0$, respectively. Complementary to the dispersion relation, the correlation length of baryon density fluctuations provides an additional measure for the size of the primary fragmentation pattern. We can estimate the correlation's length of baryon density fluctuations as the width of the correlation function at half-maximum. From the figure, we estimate that the correlation length is about the same at both densities and temperatures around 3.0 fm, which is consistent with the dispersion relation presented in Fig. 1. Baryon density fluctuations grow faster at $\rho_b = 0.4\rho_0$ than $\rho_b = 0.2\rho_0$. Figure 7 shows similar information calculated in the nonrelativistic approach [12]. The correlation length is around 3.5 fm at $\rho_b = 0.4\rho_0$ and 3.0 fm at the lower density

$\rho_b = 0.2\rho_0$. However, unlike the relativistic calculations, the baryon density fluctuations grow faster at lower density $\rho_b = 0.2\rho_0$ than at $\rho_b = 0.4\rho_0$, which is a consistent result with that presented in Fig. 2.

IV. CONCLUSIONS

It has been demonstrated in recent publications [7,9,10,12] that the stochastic mean-field approach incorporates both the one-body dissipation and the associated fluctuation mechanism in a manner consistent with the fluctuation-dissipation theorem of nonequilibrium statistical mechanics. Therefore the approach provides a powerful tool for investigating dynamics of density fluctuations in low-energy nuclear collisions. In a similar manner, it is possible to develop an extension of the relativistic mean-field theory by incorporating the initial quantal zero point fluctuations and thermal fluctuations of density in a stochastic manner. In this work, by employing the stochastic extension of the relativistic mean-field approach, we investigated spinodal instabilities in symmetric nuclear matter in the semiclassical framework. We determined the growth rates of unstable collective modes at different initial densities and temperatures. The stochastic approach also allowed us to calculate the early development of baryon density correlation functions in the spinodal region, which provides valuable complementary information about the emerging fragmentation pattern of the system. We compared the results with those obtained in nonrelativistic calculations under similar conditions. Our calculations indicated a qualitative difference in behavior in the unstable response of the system. In the relativistic approach, the system exhibited most unstable behavior at higher baryon densities around $\rho_b = 0.4\rho_0$, while in the nonrelativistic calculations most unstable behavior occurred at lower baryon densities around $\rho_b = 0.2\rho_0$. In the present exploratory work, we employed the original Walecka model without a self-interaction of the scalar meson. The qualitative difference in the unstable behavior may be partly due to the fact that the original Walecka model leads to a relatively small value of the nucleon effective mass of $M^* = 0.541M$ and a large nuclear compressibility of 540 MeV. On the other hand, the Skyrme interaction that we employ in nonrelativistic calculations gives rise to a compressibility of 201 MeV [12]. It will be interesting to carry out further investigations of spinodal dynamics in symmetric and charge asymmetric nuclear matter by including the self-interaction of the scalar meson and also including the rho meson in the calculations. The inclusion of the self-interaction of scalar meson allows us to investigate spinodal dynamics over a wide range of nuclear compressibility and nuclear effective mass. We also note by working in the semiclassical framework, we neglect the quantum statistical effects on the baryon density correlation function, which become important at lower temperatures and also at lower densities.

ACKNOWLEDGMENTS

S.A. gratefully acknowledges TUBITAK for partial support and METU for the warm hospitality extended to him during

his visit. This work is supported in part by the US DOE Grant No. DE-FG05-89ER40530 and in part by TUBITAK Grant No. 107T691. Also, it is supported in part by the

Bundesministerium für Bildung und Forschung (BMBF), Germany, under Project 06 MT 246, and by the DFG cluster of excellence “Origin and Structure of the Universe.”

-
- [1] Ph. Chomaz, M. Colonna, and J. Randrup, *Phys. Rep.* **389**, 263 (2004).
- [2] S. Ayik, M. Colonna, and Ph. Chomaz, *Phys. Lett.* **B353**, 417 (1995).
- [3] B. Jacquot, S. Ayik, Ph. Chomaz, and M. Colonna, *Phys. Lett.* **B383**, 247 (1996).
- [4] B. Jacquot, M. Colonna, S. Ayik, and Ph. Chomaz, *Nucl. Phys.* **A617**, 356 (1997).
- [5] M. Colonna, Ph. Chomaz, and S. Ayik, *Phys. Rev. Lett.* **88**, 122701 (2002).
- [6] V. Baran, M. Colonna, M. Di Tora, and A. B. Larionov, *Nucl. Phys.* **A632**, 287 (1998).
- [7] S. Ayik, *Phys. Lett.* **B658**, 174 (2008).
- [8] R. Balian and M. Veneroni, *Phys. Lett.* **B136**, 301 (1984).
- [9] S. Ayik, K. Washiyama, and D. Lacroix, *Phys. Rev. C* **79**, 054606 (2009).
- [10] K. Washiyama, S. Ayik, and D. Lacroix, *Phys. Rev. C* (2009) (in press).
- [11] H. Feldmeier, *Rep. Prog. Phys.* **50**, 915 (1987).
- [12] S. Ayik, N. Er, O. Yilmaz, and A. Gokalp, *Nucl. Phys.* **A812**, 44 (2008).
- [13] P. Ring, *Prog. Part. Nucl. Phys.* **37**, 193 (1996).
- [14] B. D. Serot and J. D. Walecka, *Int. J. Mod. Phys. E* **6**, 515 (1997).
- [15] D. Vretenar, H. Berghammer, and P. Ring, *Nucl. Phys.* **A581**, 679 (1995).
- [16] D. Vretenar, A. V. Afanasjev, G. A. Lalazissis, and P. Ring, *Phys. Rep.* **409**, 101 (2005).
- [17] S. S. Avancini, L. Brito, D. P. Menezes, and C. Providencia, *Phys. Rev. C* **71**, 044323 (2005).
- [18] A. M. Santos, L. Brito, and C. Providencia, *Phys. Rev. C* **77**, 045805 (2008).
- [19] C. Ducoin, C. Providencia, A. M. Santos, L. Brito, and Ph. Chomaz, *Phys. Rev. C* **78**, 055801 (2008).
- [20] C. H. Dasso, T. Dossing, and H. C. Pauli, *Z. Phys. A* **289**, 395 (1979).
- [21] H. Esbensen, A. Winther, R. A. Broglia, and C. H. Dasso, *Phys. Rev. Lett.* **41**, 296 (1978).
- [22] C. H. Dasso, in *Proceedings of the La Rabidia International Summer School on Theory of Nuclear Structure and Reactions*, edited by G. Madurga and M. Lozano (World Scientific, Singapore, 1986).
- [23] C. M. Ko, Q. Li, and R. Wang, *Phys. Rev. Lett.* **59**, 1084 (1987).
- [24] E. M. Lifshitz and L. P. Pitaevskii, *Physical Kinetics* (Butterworth-Heinemann, 1981).
- [25] P. Bozek, *Phys. Lett.* **B383**, 121 (1996).